S.S. I

Contents lists available at ScienceDirect

## **Extreme Mechanics Letters**

journal homepage: www.elsevier.com/locate/eml



# A method to compute elastic and entropic interactions of membrane inclusions



Xiaojun Liang, Prashant K. Purohit \*

Department of Mechanical Engineering and Applied Mechanics, University of Pennsylvania, Philadelphia, PA 19104, United States

#### ARTICLE INFO

Article history:
Received 10 July 2017
Received in revised form 23 October 2017
Accepted 31 October 2017
Available online 10 November 2017

Keywords: Membrane inclusions Elastic plate model Lipid bilayer Entropic forces

#### ABSTRACT

Curvature mediated elastic interactions between inclusions in lipid membranes have been analyzed using both theoretical and computational methods. Entropic corrections to these interactions have also been studied. Here we show that elastic and entropic forces between inclusions in membranes can compete under certain conditions to a yield a maximum in the free energy at a critical separation. If the distance between the inclusions is less than this critical separation then entropic interactions dominate and there is an attractive force between them, while if the distance is more than the critical separation then elastic interactions dominate and there is a repulsive force between them. We assume the inclusions to be rigid and use a previously developed semi-analytic method based on Gaussian integrals to compute the free energy of a membrane with inclusions. We show that the critical separation between inclusions decreases with increasing bending modulus and with increasing tension. We also compute the projected area of a membrane with rigid inclusions under tension and find that the trend of the effective bending modulus as a function of area fraction occupied by inclusions is in agreement with earlier results. Our technique can be extended to account for entropic effects in other methods which rely on quadratic energies to study the interactions of inclusions in membranes.

© 2017 Elsevier Ltd. All rights reserved.

### 1. Introduction

In mechanics, the forces of interaction between defects in an elastic body are well understood. For example, two screw dislocations with Burger's vectors b and b' at a distance r from each other interact with a force per unit length f of magnitude f $\mu bb'/(2\pi r)$  where  $\mu$  is the shear modulus of the solid. This interaction force arises because the defects produce elastic fields around them which can overlap. The interaction between the defects could be attractive or repulsive depending on whether the total elastic energy of the solid decreases or increases due to the overlapping of stress and strain fields produced by the defects [1]. Interactions between defects in an elastic solid can also arise due to entropic effects. For example, the equilibrium concentration of vacancies in a solid is a result of the competition between the elastic energy and the entropy of the vacancies. The elastic part of the free energy of the solid,  $U_{el}$ , increases if the vacancy concentration increases because the vacancies create elastic fields around them that store energy. On the other hand, the entropic part of the free energy of the solid  $U_{en} = -TS \approx -T(c \log c + (1-c) \log(1-c))$  decreases as the vacancy concentration c increases, for  $c \ll 1$ . This competition gives rise to a non-zero vacancy concentration at which the free energy is a minimum [2]. In a similar vein, the chemical force on a dislocation has its origins in the entropy of vacancies [1]. The physics of elastic and entropic interactions described above is applicable to any kind of defect of in an elastic material. Since lipid membranes can be modeled as elastic continua we will apply concepts similar to those described above to inclusions, such as proteins, in them.

If two similar proteins bind to a lipid bilayer separated by a distance r then the elastic deformation field around one of them can produce a repulsive force on the other one [3]. The potential of this force decays as  $1/r^4$  as has been deduced from studies of proteins interacting through elastic deformations of a lipid bilaver [4– 10l. Lipid membranes also fluctuate due to Brownian motion. This results in an attractive entropic force between two similar proteins [4,6]. The competition between attractive and repulsive forces can lead to self-assembly of proteins on a lipid bilayer membrane [11,12]. This sort of self-assembly determines the shape of a cell membrane and plays a role in endo- and exo-cytosis by the formation of localized invaginations or buds. Bud formation is exactly what happens when capsid proteins of viruses, like HIV and influenza, land on lipid membranes and self-assemble [4]. Similarly, the protein endophilin clusters together on lipid membranes and causes the formation of cylindrical tubules, and thus, it plays a role in membrane trafficking events in a cell [13]. The early stages of self-assembly of certain amyloid forming proteins (which cause

<sup>\*</sup> Corresponding author.

E-mail address: purohit@seas.upenn.edu (P.K. Purohit).

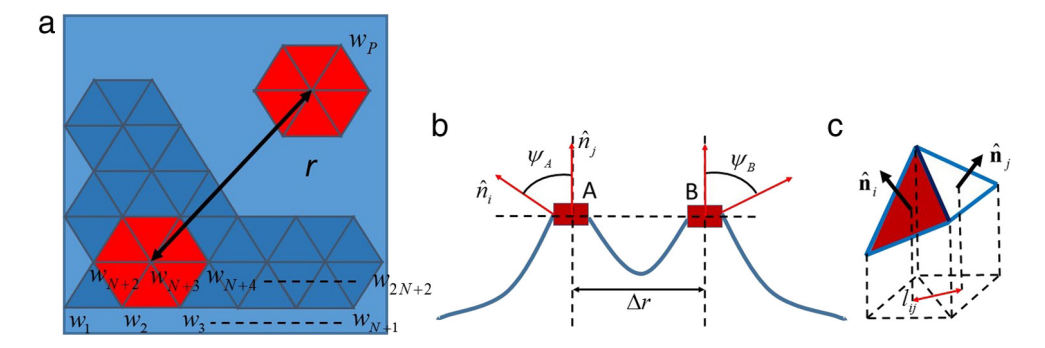


**Fig. 1.** (a) Equilateral triangle element discretization scheme of a square membrane. The inclusions are represented by red hexagons consisting of many triangle elements. We keep the element size fixed, so the number of triangle elements in an inclusion depends on the size of the inclusion. (b) The equilibrium shape of a membrane with two proteins embedded in it and separated by a distance  $\Delta r$ . The proteins are rigid cylinders which enforce contact angles  $\psi_A$  and  $\psi_B$  with respect to the adjacent membrane. In section 3.1, we will fix these angles to a given value as an enforced boundary condition. (c) Unit normal vectors  $\hat{n}_i$  and  $\hat{\eta}_j$  of two elements sharing one inclusion—membrane boundary edge.  $I_{ij}$  is the reference length between the center of these two triangle elements. The red triangle belongs to the inclusion. (For interpretation of the references to color in this figure legend, the reader is referred to the web version of this article.)

Alzheimer's and Parkinson's diseases) also involves self-assembly of monomers on a lipid membrane [14]. Since self-assembly often involves many more than two proteins, the interactions between many proteins on a membrane have been studied and it has been learned that pair-wise expressions are not sufficient to describe these many body interactions [5]. However, most analytic studies of these many body interactions account for membrane bending deformations only. The entropic component of the interactions has been studied recently using simulations and a sophisticated field theory [6,7]. The field theory relies on the idea that the height fluctuations of the membrane are small, so the bending energy can be written as a quadratic form. This leads to Gaussian path integrals that can be evaluated analytically, but not without difficulty [6].

Our overarching goal here is to study elastic and entropic forces between many inclusions on lipid membranes using computational methods based on Gaussian integrals. Although mechanical and thermodynamic properties of lipid membranes, including how inclusions (such as, proteins) effect the overall membrane behavior, have been quantitatively studied using experimental, theoretical and computational methods [15-22], it is not always possible to design an experiment for large scale problems involving membrane protein interactions; on the other hand, the sample scale is too large for molecular simulations. To overcome these difficulties, researchers have turned to continuum modeling and associated computational methods [23] to study large scale (more than several microns) problems involving protein interactions on membranes. Unlike molecular simulation (such as, Monte Carlo and Molecular Dynamics based studies [21,22]) these continuum methods do not include Brownian fluctuations. Our technique described below can potentially be combined with continuum computational methods to account for entropic effects arising from Brownian fluctuations.

## 2. Theory

## 2.1. Semi-analytic method to compute membrane free energy

The thermodynamic properties of a fluctuating lipid membrane have been studied by starting from an energy expression [24,25]:

$$E_b = \int_0^L \int_0^L \mathrm{d}x \mathrm{d}y \left\{ \frac{K_b}{2} \left( w_{,xx} + w_{,yy} \right)^2 + \frac{F}{2} (w_{,x}^2 + w_{,y}^2) \right\}. \tag{1}$$

Here, L is the side of a square membrane,  $K_b$  is the bending modulus, and F is the externally applied isotropic tension. The variable w(x,y) in the expression above is the out-plane deflection of the neutral plane. We assume that the deformation is relatively small such that there are no overhangs in the membrane, and thus the

displacement of each point is written as a function of the in-plane coordinate (x, y). We discretize the membrane into approximately  $Q = 4N^2/\sqrt{3}$  equilateral triangle elements of side l as shown in Fig. 1(a) (so that N = L/l), similar to many Monte Carlo simulations on other fluid and solid membranes [26,27]. But, in contrast to the Monte Carlo simulations we will compute the partition function analytically. The key idea is to express the membrane energy quadratically as a function of approximately  $P \approx 2N(N+1)/\sqrt{3}$  node variables  $w_i$ , i = 1..P as in [24,25]:

$$E = \frac{4K_b A_e}{3l^4} \sum_{(i,j)} (w_i + w_j - w_k - w_l)^2 + \frac{FA_e}{3l^2} \sum_{(i,j)} [(w_r - w_s)^2 + (w_s - w_t)^2 + (w_t - w_r)^2].$$
(2)

Here the summation in the bending energy term runs over all the adjacent triangle element pairs that share one edge linked by nodes i. i. with k. l. being the other two nodes of these two elements. The summation in the potential energy of the tension F runs over all the triangle elements. The subscripts r, s, t denote the nodes of one triangle in the second sum,  $A_e = L^2/Q$  is the reference area of one triangle. Since the energy expression is quadratic, we can define a stiffness matrix **M** such that  $E = \mathbf{w}\mathbf{M}\mathbf{w}^{\mathrm{T}}$ , where the vector  $\mathbf{w} = [w_1, w_2, \dots, w_P]$  contains all the node displacements. Recall that **M** is a function of  $K_b$ , F, L, l. In statistical mechanics,  $\frac{1}{7} \exp(-E/k_BT)$  is the probability of finding a system in a given state of energy E, where  $k_B$  is the Boltzmann constant, T is the absolute temperature and Z is the partition function. Next, we are going to compute the partition function Z by carrying out the integration of exp  $(-E/k_BT)$  over all possible states of the system as in [28-31]. The partition function Z scales inversely with the square root of the determinant of M, as

$$Z = \sqrt{\frac{(2\pi k_B T)^P}{\det \mathbf{M}}}.$$
 (3)

The Gibbs free energy G(F,T) of the membrane is related to the partition function Z as  $G=-k_BT\ln Z$ , and hence the projected area, entropy and other thermal quantities can be computed by differentiating G(F,T). We computed the projected area and entropy of the membrane as a function of T,  $K_b$  and F using the method above in [24] and recovered results from well-known analytic expressions for the projected area [18] and entropy in the limit as I became small. For I = 1  $\mu$ m and 0.01 pN/nm I = 2.5 nm resulted in excellent agreement with the known analytic formula for projected area and entropy. Thus, we have the capability to capture elastic and entropic effects in fluctuating membranes.

#### 2.2. A model for inclusions

A lipid bilayer membrane in a live cell has proteins embedded in it, whose size is a few nanometers. These proteins are much stiffer than lipid molecules and they have strong interactions with their surrounding lipids [32]. The embedded proteins change the local shape of the membrane and affect both the elastic and entropic parts of the membrane free energy. We will now apply our semi-analytic method described above to the study the effect of membrane inclusions. We model each inclusion by assigning some of the triangle elements with much larger bending stiffness (10<sup>3</sup> pNnm for all computations in this paper) than the lipid membrane as shown in Fig. 1(a). Also, we fixed the displacement of all the inclusion nodes to be zero to compute the bending energy. Thus, we are assuming the inclusions to be rigid disks in comparison to the membrane. An advantage of assuming rigid inclusions is that we do not have to account for the energy due to Gauss curvature in our calculations [5]. One inclusion could contain 6, 24, or 54 equilateral triangle elements depending on its size. The inclusionmembrane interaction at the boundary of each inclusion (labeled  $A, B, \ldots$ ) is modeled by uniform contact angles  $\psi_A, \psi_B, \ldots$  Here  $\psi_A$ is the angle between the boundary triangle elements of inclusion A and the adjacent membrane triangle elements shown in Fig. 1(b). If we remember that the displacement of all nodes on the inclusions is zero then the displacement of inclusion-adjacent membrane nodes is  $w = \frac{\sqrt{3}}{2}l\sin\psi_A$  at T = 0. Since all our boundary conditions are specified node displacements we solve for the displacements of all other nodes comprising the membrane using standard techniques in the finite element method (see, for example, [33]). Once the displacements of all nodes are known the elastic energy can be immediately computed using Eq. (2). To compute the entropic contribution to the free energy we add a penalty energy  $E_p$  to Eq. (2), as is done in earlier works [25,28]. Here the penalty energy is written as the sum:

$$E_p = \lambda \sum_{C} (\psi - \psi_A)^2, \tag{4}$$

where  $\psi_A$  is chosen to be 0.1 for all computations, and  $\lambda$  is a penalty energy coefficient, which is chosen to be large enough (e.g.  $\lambda=10^{12}$  in [25]) to ensure that the probability of configurations violating the boundary condition is extremely small in the partition sum for Z. The contour C is the boundary of all the proteins, thus we have tacitly assumed that all proteins have the same contact angle with the membrane. We can, of course, impose a different contact angle at every protein, but we do not do so here for simplicity.  $\psi$  could be expressed as the absolute value of the difference between unit normal vectors  $\hat{n}_i$ ,  $\hat{n}_j$  of the two elements sharing one boundary edge as in Fig. 1(c), or

$$\psi = |\hat{n}_i - \hat{n}_i|. \tag{5}$$

Recall that  $\hat{n}_i$  and  $\hat{n}_j$  can be represented by quadratic expressions of node displacement variables  $[w_1, w_2, \ldots, w_P]$ . Therefore, we can write the penalty energy by an algebraic expression

$$E_p = \mathbf{w} \mathbf{M}_{\mathbf{P}} \mathbf{w}^{\mathrm{T}} + \mathbf{w} \cdot \mathbf{C}_{\mathbf{p}} + C, \tag{6}$$

where  $C_p$  is a vector and C is a constant. Now, we perform the same exercise as in [24]; we replace the stiffness matrix M in Eq. (3) with a new matrix  $M + M_P$  taking care of both membrane energy as well as penalty energy, and rewrite the energy expression as:

$$E + E_p = (\mathbf{w} - \bar{\mathbf{w}}) (\mathbf{M} + \mathbf{M_P}) (\mathbf{w} - \bar{\mathbf{w}})^{\mathrm{T}} + \bar{C}$$
(7)

where the equilibrium position  $\bar{\mathbf{w}}$  has been computed before by enforcing displacement boundary conditions at each inclusion and  $\bar{C}$  is a constant taking care of the equilibrium position energy. Finally, we carry out the integral for the partition function:

$$Z = \exp\left(-\frac{\bar{C}}{k_B T}\right) \sqrt{\frac{\left(2\pi k_B T\right)^P}{\det\left(\mathbf{M} + \mathbf{M_P}\right)}}.$$
 (8)

The membrane free energy with inclusions is thus given by:

$$G = -k_B T \ln Z = \bar{C} + \frac{k_B T}{2} \ln \det (\mathbf{M} + \mathbf{M_P}) + G_0.$$
 (9)

Here the first term takes care of the elastic contribution which is independent of temperature, and the second term takes care of the entropic contribution, which increases linearly with temperature, and  $G_0$  is a constant.

Although we used the penalty energy formulation above due to the simplicity of implementing it, we must point out a pitfall and alternative methods to account for the constraints in our calculation of the entropic contribution to the free energy. The caveat in introducing an extraneous parameter  $\lambda$  (the penalty parameter in Eq. (4) above) is that the free energy will now depend on  $\lambda$  too, which is unphysical. To avoid this difficulty we plot the variance of the fluctuations in **w** as a function of  $\lambda$  and choose  $\lambda$  so large that the variance is practically independent of  $\lambda$ . An example of such a plot can be found in Fig. 3(c) of [25]. Now, there are other ways of accounting for constraints without introducing an extraneous  $\lambda$ . One such method is (a) to incorporate the constraints into the partition sum through a  $\delta$ -function which enforces the counting of only those configurations that satisfy the constraint, then (b) express the  $\delta$ -function through Fourier transform as  $\delta(x) =$  $\frac{1}{2\pi} \int_{-\infty}^{\infty} e^{ikx} dk$ , and then (c) use the saddle-point approximation to compute the integral for the partition function [28]. Yet another method that can be used for special situations involves (a) eliminating some degrees of freedom using the constraint equations, (b) approximating the energy for the configurations satisfying the constraints to quadratic order in the remaining degrees of freedom, and (c) using Gaussian integrals to compute the partition function by integrating over these remaining degrees of freedom. We have used the 'penalty method' to compute the partition function here because it is well-established as a method of imposing constraints in finite element calculations (see, for example, [33]).

#### 3. Results

#### 3.1. Interaction of two inclusions

The first problem solved using our method is to compute the interactions between two proteins on a lipid bilayer as shown in Fig. 1(a). We can compute both the elastic and entropic parts of the free energy of this lipid membrane as a function of a protein separation distance r. We choose a membrane with side L =500 nm and a discretization scheme with N = 200, resulting in an element size l=2.5 nm because it resulted in excellent agreement between our computations and the analytic expressions for membrane entropy [24]. The bending modulus is varied from  $5k_BT$  to  $20k_BT$  and membrane tension is set to zero. We hinge all four sides of the membrane. The inclusions contain 6, 24, or 54 equilateral triangle elements depending on their radius R. The results for various computation groups in Table 1 are shown in Fig. 2. In each plot the distance r is on the x-axis, the elastic part of the free energy (blue curve and circles) is on the left y-axis and the entropic part of the free energy (green curve and circles) is on the right y-axis.

We see in all the computation groups that the entropic part of the free energy increases with protein separation distance and the elastic part decreases with protein separation distance. The

<sup>&</sup>lt;sup>1</sup> This is by assuming  $\psi$  to be small such that  $\cos \psi = 1 - \psi^2/2$ . Therefore,  $|\hat{n}_i - \hat{n}_j|^2 = 2 - 2\hat{n}_i \cdot \hat{n}_j = 2 - 2\cos \psi = \psi^2$ .

**Table 1**Parameters used in the two inclusion computations.

Group	L(nm)	Element size(nm)	$K_b$ (pNnm)	Inclusion radius (nm)	a <sub>el</sub> (pNnm <sup>5</sup> )	a <sub>en</sub> (pNnm <sup>5</sup> )	r <sub>cr</sub> (nm)
A	500	2.5	82	7.5	$5.86 \times 10^{5}$	$-8.72 \times 10^{5}$	_
В	500	2.5	41	7.5	$2.93 \times 10^{5}$	$-9.41 \times 10^{5}$	-
C	500	2.5	20.5	7.5	$1.46 \times 10^{5}$	$-9.97 \times 10^{5}$	-
D	500	2.5	82	5	$2.25 \times 10^{5}$	$-1.40 \times 10^{4}$	-
E	500	2.5	41	5	$1.12 \times 10^{5}$	$-1.69 \times 10^{4}$	-
F	500	2.5	20.5	5	$5.56 \times 10^{4}$	$-1.87 \times 10^{4}$	-
G	500	2.5	82	2.5	$6.21 \times 10^{4}$	$-1.97 \times 10^{3}$	-
Н	500	2.5	41	2.5	$3.11 \times 10^{4}$	$-2.13 \times 10^{3}$	-
I	500	2.5	20.5	2.5	$1.55 \times 10^{4}$	$-2.23 \times 10^{3}$	-
J	500	2.5	6.15	2.5	$4.66 \times 10^{3}$	$-2.31 \times 10^{3}$	25
K	500	2.5	4.1	2.5	$3.11 \times 10^{3}$	$-2.33 \times 10^{3}$	30
L	500	2.5	3.28	2.5	$2.49 \times 10^{3}$	$-2.33 \times 10^{3}$	35
M	500	2.5	2.87	2.5	$2.18 \times 10^{3}$	$-2.28 \times 10^{3}$	40

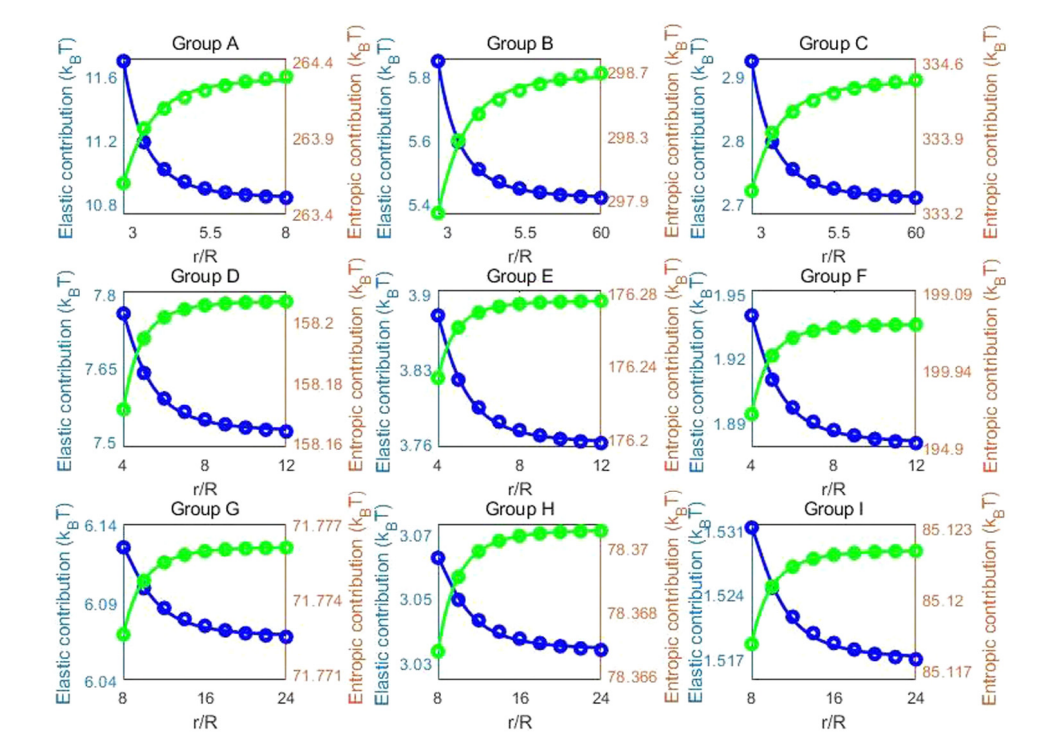


**Fig. 2.** Results for computations with two inclusions on a membrane with properties summarized in Table 1. Circles are computation results and solid lines are theoretical fits using Eq. (10). Blue and green data, associated with left and right y-axis respectively, correspond to elastic and entropic parts of the membrane free energy is non-dimensionalized by  $k_BT$  at 300 K, and inclusion separation distance r is non-dimensionalized by inclusion radius R. (For interpretation of the references to color in this figure legend, the reader is referred to the web version of this article.)

dependence of both entropic and elastic parts of the free energy has been studied analytically in [6] and references therein. It is known that the elastic and entropic parts of the free energy of a membrane with two identical rigid circular disks whose centers are a distance r apart take the form (to lowest order in 1/r):

$$U_{el}(r) = \frac{a_{el}}{r^4} + O(\frac{1}{r^6}),$$

$$U_{en}(r) = \frac{a_{en}}{r^4} + O(\frac{1}{r^6}).$$
(10)

The subscript  $_{el}$  and  $_{en}$  indicate elastic and entropic parts, respectively. We obtained  $a_{el}$  and  $a_{en}$  by fitting each computation group in Table 1 using Eq. (10) as shown by the solid lines in Fig. 2. According to Yolcu et al. [6] the  $r^{-6}$  term in the elastic part of the free energy is zero for two circular inclusions of the same radius R, so we did not include this term in our fits for  $U_{el}(r)$ . The fitting parameter  $a_{el}$  should scale with  $K_b\psi_A^2R^4$ , while fitting parameter  $a_{en}$  should scale with  $k_BTR^4$  and be independent of  $K_b$  if the inclusions are circular disks of radius R as in [6]. In Fig. 3 we see that our  $a_{el}$  (solid

lines) increases linearly with bending modulus  $K_b$ , and  $a_{en}$  (dashed lines) remains almost unchanged as bending modulus increases from  $5k_BT$  to  $20k_BT$ , which agrees with the analytic theory based on Gaussian integrals [6]. We see from Table 1 that the magnitudes of  $a_{el}$  and  $a_{en}$  increase with inclusion size, as expected. We do not expect exact agreement of our computations with [6] because (a) our inclusions are hexagonal in shape while those in [6] are circular, (b) we use only the first few terms in the expansions provided in [6] to fit our results, (c) our membrane is not infinite as in [6] and has specific boundary conditions applied at its edges, and (d) the expansions in [6] are valid, presumably, for  $R/r \ll 1$ , while for some of our computations R/r < 1.

## 3.2. Free energy maxima due to elastic entropic competition

Fig. 2 shows that the elastic and entropic parts of the free energy have opposing trends as functions of r,  $U_{el}(r)$  decreases as r increases, and  $U_{en}$  increases as r increases. This competition could result in a maximum in the total free energy if the appropriate

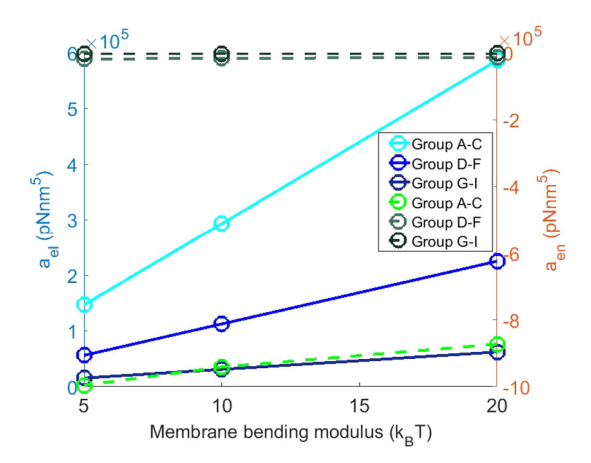


**Fig. 3.** Dependence of fitting parameters  $a_{el}$  and  $a_{en}$  in Eq. (10) on membrane bending modulus and inclusion size. The blue solid lines associated with the left y-axis are results for  $a_{el}$ , which increases linearly with  $K_b$ . The green dashed lines associated with the right y-axis are results for  $a_{en}$ , which are almost independent of  $K_b$  ( $a_{en}$  decreases very slowly with decreasing  $K_b$ ). (For interpretation of the references to color in this figure legend, the reader is referred to the web version of this article.)

system parameters are chosen. Fig. 2 shows that if we choose  $\psi_A =$ 0.1 then for most lipid bilayer membranes the elastic contribution dominates the entropic contribution and there is no extremum in the free energy. However, while the entropic contribution is independent of  $K_b$  the elastic contribution can be made smaller by lowering  $K_b$  so that the two balance to give an extremum. To test this idea, we chose lower bending moduli  $K_b = 0.7 - 1.5 k_B T$  (Group J-M in Table 1) and computed the free energy of our membrane with two inclusions of radius 2.5 nm at zero tension. Such low bending moduli are known to occur for surfactant membranes (see [34] and references therein). Note from Table 1 that the fitted values of  $a_{en}$  do not vary much for this group of computations while the fitted values of  $a_{el}$  vary linearly with  $K_b$ . In Fig. 4(a) we plot the free energy U(r) for two of these membranes and see a maximum in each case. In fact,  $a_{el} \propto K_b \psi_A^2$  where  $\psi_A$  is the boundary contact angle at the inclusion [6], so the maximum can also be obtained by varying  $\psi_A$  instead of  $K_b$ . Let us label the inter-inclusion separation r at the maximum by  $r_{cr}$ . The sign of  $\frac{dU}{dr}$  indicates that for  $r < r_{cr}$ the interaction force between the inclusions is attractive, while for  $r > r_{cr}$  the interaction force is repulsive.

The location of the maximum,  $r_{cr}$ , decreases with increasing  $K_b$  as shown in the inset of Fig. 4(a). This may be qualitatively understood as follows. For  $K_b = 0$  the free energy is entirely entropic and tends to a maximum as  $r \to \infty$ , while for large  $K_b$  when the elastic energy dominates the entropy (i.e.,  $a_{el} \gg -a_{en}$ ) the free energy tends to a maximum as  $r \to 0$ . Hence, as  $K_b$ 

decreases we expect  $r_{cr}$  (the location of the maximum in the free energy) to increase. In our calculation, we cannot find the exact location of the maximum,  $r_{cr}$ , since we only choose the separation distances that are multiples of l, the element size. However, we are able to see the trend of  $r_{cr}$  increasing as the bending modulus of the membrane  $K_b$  decreases.

In order to ensure that the maximum obtained in our calculations above is real and not an artifact of computation we verify below that it can also be found by going back to the asymptotic expressions for  $U_{el}(r)$  and  $U_{en}(r)$  given in Yolcu et al. [6] for two circular inclusions of radius R. For the entropic part of the free energy the first five terms in Yolcu et al. [6] are:

$$U_{en}(r) = -k_B T \left( \frac{6}{x^4} + \frac{20}{x^6} + \frac{84}{x^8} + \frac{344}{x^{10}} + \frac{1388}{x^{12}} + \cdots \right), \tag{11}$$

where  $x=\frac{r}{R}$ . This gives an entropic interaction force that is attractive for all r>0. We have argued above that addition of an elastic energy  $U_{el}(r)$  could result in a maximum in the free energy which would make the interaction force repulsive for  $r>r_{cr}$ . To see if this is true we consider the asymptotic expansion of  $U_{el}(r)$  given in [6]:

$$U_{el}(r) = \frac{8\pi K_b \psi_A^2}{x^4} + O(\frac{1}{x^6}). \tag{12}$$

We plotted  $U(r) = U_{el}(r) + U_{en}(r)$  as a function of r and confirmed that the shape of the curves is similar to those obtained from our computations (plots not shown). When we chose  $K_b = 20k_BT$  and  $\psi_A = 0.11$  then the maximum was at  $\frac{r_{cr}}{R} = 19.1$  (or  $r_{cr} = 47.8$  nm if R = 2.5 nm) and for  $K_b = 21k_BT$  and  $\psi_A = 0.11$  the maximum moved to  $\frac{r_{cr}}{R} = 8.82$  (or  $r_{cr} = 22$  nm if R = 2.5 nm). These calculations confirmed that the trends from our computational method described above are not artifacts.

## 3.3. Effect of tension on free energy maxima

While changing the bending modulus  $K_b$  or boundary angle  $\psi_A$  is one way of controlling the magnitude of elastic and entropic parts of the free energy, another way to do so is to change the hydrostatic tension. We have tried this for  $K_b = 0.9k_BT$  by applying a tension  $F = 1 \times 10^{-5}$  pN/nm to  $F = 5 \times 10^{-3}$  pN/nm (Group N-P in Table 2). In Fig. 4(b), we compare the computation result of total free energy of Group N and P of same bending modulus  $K_b$ . The non-zero value of tension increases the elastic part of the free energy because the potential energy of the applied tension is added. It decreases the entropic contribution since tension stretches out the ripples of out-of-plane thermal fluctuation. The net result is that the location of the free energy maxima  $r_{cr}$  decreases with increasing F, and thus Fig. 4(a) and (b) exhibit a similar result.

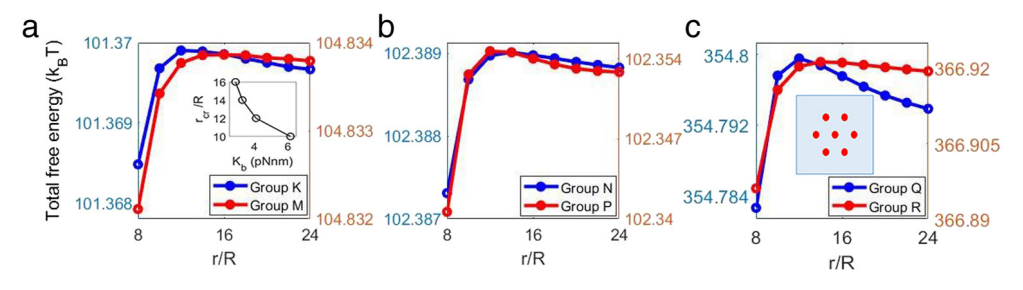


**Fig. 4.** Non-dimensionalized total free energy profile of selected groups in Tables 1 and 2. (a) The position of the maximum  $r_{cr}$  moved to the left as bending modulus increased. (b) The position of the maximum  $r_{cr}$  moved to the left as bending modulus increased for a cluster of seven proteins. The blues lines and red lines are associated with left and right *y*-axis respectively. The inset in (a) shows the position of the maximum,  $r_{cr}$ , as a function of  $K_b$  for zero tension as (see group J–M in Table 1) as dots. The inset in (c) show the layout of protein clusters. (For interpretation of the references to color in this figure legend, the reader is referred to the web version of this article.)

**Table 2**Parameters used in the cluster computations.

Group	L(nm)	Element size(nm)	K <sub>b</sub> (pNnm)	Inclusion radius (nm)	Number of inclusions	tension F (pNnm <sup>-1</sup> )	r <sub>cr</sub> (nm)
N	500	2.5	3.69	2.5	2	0.00001	35
0	500	2.5	3.69	2.5	2	0.0005	35
P	500	2.5	3.69	2.5	2	0.005	30
Q	500	2.5	4.1	2.5	7	0	30
R	500	2.5	2.87	2.5	7	0	35
S	500	2.5	2.87	2.5	7	0.01	40

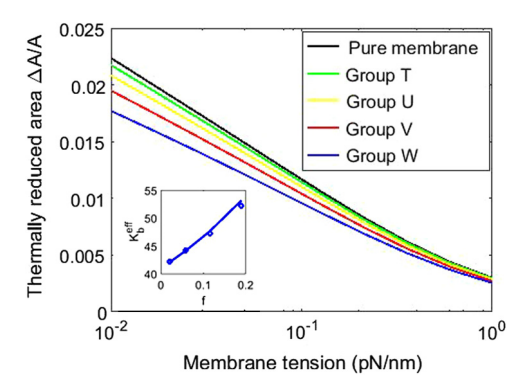


**Fig. 5.** Thermally reduced area change vs. membrane tension for various area fractions of membrane inclusions. The inset shows effective membrane bending modulus vs. membrane inclusion fractions (dots), fitted by a line given by Eq. (14).

#### 3.4. Cluster of inclusions

Having benchmarked our computations against analytic results we want to go beyond pair-wise interactions which are known not to apply to many-body interactions [5]. Our computational method is not restricted to just two inclusions; it can equally well be used to study interactions between many inclusions in a membrane. To illustrate the capability of our method we will assume that a cluster of seven inclusions forms a regular hexagon with one inclusion at each of the six vertices and one at the center as shown in the inset of Fig. 4(c). The side of the hexagon is r. Our choice of parameters for the membrane inclusion system is shown in Table 2. We compute the total free energy of the system as a function of r and change both  $K_b$  and F in computation groups Q. R and S. For all groups we see a maximum in the free energy, as shown in Table 2 and plotted in Fig. 4(c). If  $r < r_{cr}$  then these proteins will attract each other due to entropic interactions and r will decrease until a preferred separation is dictated by short range interactions. The value of  $r_{cr}$  can be modulated by changing the tension F. A more detailed analysis (including a parameter study) of such clusters of inclusions is left to future work, but the computations presented here suffice to illustrate the capabilities of our computational method.

#### 3.5. Thermally reduced area change affected by inclusions

Out-of-plane thermal fluctuation of a lipid membrane results in a shrinking of the membrane projected area. From [18–20], the projected area  $A - \Delta A$  of a lipid membrane of area A (reference area at T=0) and no inclusions is related to the membrane bending modulus and membrane tension as:

$$\frac{\Delta A}{A} = \frac{k_B T}{8\pi K_b} \ln \frac{\pi^2 / b^2 + F / K_b}{\pi^2 / A + F / K_b},\tag{13}$$

where *b* is the radius of a lipid head group and is on the order of 1 nm. If stiff proteins bind to a membrane, its thermal fluctuation should be suppressed and thus result in a larger projected area than a membrane with no inclusions, We will now determine how

this change quantitatively depends on the protein area fraction f. According to [22], there is an effective bending modulus as a function of f given by

$$K_b^{eff} = \frac{K_b}{1 - cf},\tag{14}$$

where c is a coefficient affected by system properties, which could be obtained by fitting the experimental or simulation data. In our finite element model, we can test the effect of stiff proteins on the projected area. We choose a 250 nm  $\times$ 250 nm membrane with bending modulus  $K_b = 10k_BT$  and tension ranging from 0.01-1 pN/nm with different numbers of 7.5 nm radius hexagonal inclusions as shown in Table 3. We compute the projected area change following the procedure in our previous work [24] and extract the effective bending modulus from the slope of a plot of  $\frac{\Delta A}{A}$  vs.  $\log F$ . The data are tabulated in Table 3 and the results from our computations are plotted in Fig. 5. We see that as the fraction f of inclusions increases, the change in projected area  $\Delta A$  decreases. The slope of the line plotting  $\Delta A/A$  vs.  $\log F$  increases indicating a larger effective bending modulus. We fitted this line using Eq. (13) and extracted an effective bending modulus  $K_b^{eff}$  as a function of f. A plot of  $K_b^{eff}$  as a function of f is shown in the inset of Fig. 5 along with a fit using Eq. (14) which yields c = 1.2.

#### 4. Conclusions

The main objective of this paper is to demonstrate a method which can be used to compute the elastic and entropic interactions between inclusions in lipid membranes. Our method produces results that are consistent with earlier work showing that elastic interaction energy decreases and the entropic interaction energy increases as the distance between the inclusions increases. We have also shown how the competition between elastic and entropic forces can result in a maximum in the free energy, both for two inclusions and a cluster of seven inclusions arranged on a hexagon. The position of the maximum can be modulated by changing the membrane tension, membrane bending modulus, or the contact angle between the inclusion and the lipid. The presence of a maximum in the interaction free energy implies that when the spacing between the inclusions is less than that at the maximum there will be attractive forces between the inclusions and their final arrangement will be determined by short range interactions.

Even though we have demonstrated some capabilities of our method a large parameter space remains unexplored. For example, we only considered inclusions that are hexagonal and of the same size; recent work by Kahraman et al. [23] shows that the final configuration of a cluster of proteins on a membrane depends on their shape. We did not vary the contact angle  $\psi_A$  or consider other types of boundary condition. These are also expected to affect the interaction free energy of inclusions. For example, the elastic interaction energy should be much smaller if the inclusion–membrane boundary is a hinge. A limitation of our computational method is that all the equilateral triangular elements are of the same size; ideally, the mesh should be more refined near the inclusion. The impediment to applying this idea is that it is not clear to us how to compute the membrane entropy with a non-uniform mesh. Finally,

**Table 3**Parameters used in projected area change computations.

Group	L(nm)	Element size(nm)	$K_b$ (pNnm)	Inclusion radius	Number of inclusions	Fraction f	$K_b^{eff}$ (pNnm)
T	250	2.5	41	7.5	9	0.0211	42.18
U	250	2.5	41	7.5	24	0.0587	44.12
V	250	2.5	41	7.5	49	0.115	47.24
W	250	2.5	41	7.5	81	0.191	52.21

our inclusions are assumed to be rigid; this assumption can be relaxed in our computations if we properly account for the energy due to Gauss curvature. We hope to address these topics in the near future.

The interactions between the inclusions described here fall under the category of 'curvature mediated' interactions. Interactions between inclusions in lipid membranes can arise also due to 'bilayer thickness' mediated interactions. We have not considered this second set of interactions here, but we know that they too can lead to a preferred lattice spacing between inclusions on a lipid membrane as summarized in recent work by Kahraman et al. [23]. They minimize an energy that is quadratic in u/a and its gradients where u(x, y) is half the bilayer thickness and a is half the unperturbed bilayer thickness. We believe that our methods of computing the partition function summarized here can be extended to this type of energy. Such a modification would more accurately capture the physics of interactions between inclusions in a lipid bilayer. Another important ingredient that leads to a preferred spacing between inclusions, such as proteins, on membranes is the interfacial energy at the protein's boundary with the membrane as shown by Agrawal et al. [22]. In the work of [22] the interfacial energy is assumed to depend quadratically on the jumps in displacement and slope at the protein-membrane boundary, and moduli characterizing this interfacial energy are extracted from molecular simulations of proteins embedded in lipid membranes. Once again, since the energies in this method are also quadratic in the displacements our technique can potentially be applied to obtain entropic corrections.

#### Acknowledgments

We acknowledge partial support from the National Science Foundation through grants NSF DMR 1505662 and NSF CMMI 1662101.

#### References

- Johannes Weertman, Julia Randall Weertman, Elementary dislocation theory. 1992.
- [2] John Wyrill Christian, The Theory of Transformations in Metals and Alloys, Pergamon Press, Oxford, U.K., 2002.
- [3] Ramin Golestanian, Mark Goulian, Mehran Kardar, Fluctuation-induced interactions between rods on a membrane, Phys. Rev. E 54 (6) (1996) 6725.
- [4] Teresa Ruiz-Herrero, Michael F. Hagan, Simulations show that virus assembly and budding are facilitated by membrane microdomains, Biophys. J. 108 (3) (2015) 585–595.
- [5] K.S. Kim, John Neu, George Oster, Curvature-mediated interactions between membrane proteins, Biophys. J. 75 (5) (1998) 2274–2291.
- [6] Cem Yolcu, Robert C. Haussman, Markus Deserno, The effective field theory approach towards membrane-mediated interactions between particles, Adv. Colloid Interface Sci. 208 (2014) 89–109.
- [7] Martin Michael Müller, Markus Deserno, Cell model approach to membrane mediated protein interactions, Prog. Theor. Phys. Suppl. 184 (2010) 351–363.
- [8] Yonatan Schweitzer, Michael M. Kozlov, Membrane-mediated interaction between strongly anisotropic protein scaffolds, PLoS Comput. Biol. 11 (2) (2015) e1004054.

- [9] Hongyan Yuan, Changjin Huang, Sulin Zhang, Membrane-mediated interdomain interactions, Bio. Nano. Science 1 (3) (2011) 97–102.
- [10] Changjin Huang, Hongyan Yuan, Sulin Zhang, Coupled vesicle morphogenesis and domain organization, Appl. Phys. Lett. 98 (4) (2011) 043702.
- [11] Paul G. Dommersnes, Jean-Baptiste Fournier, The many-body problem for anisotropic membrane inclusions and the self-assembly of saddlei defects into an egg cartoni, Biophys. J. 83 (6) (2002) 2898–2905.
- [12] Benedict J. Reynwar, Gregoria Illya, Vagelis A. Harmandaris, Martin M. Müller, Kurt Kremer, Markus Deserno, Aggregation and vesiculation of membrane proteins by curvature-mediated interactions, Nature 447 (7143) (2007) 461– 464.
- [13] Khashayar Farsad, Niels Ringstad, Kohji Takei, Scott R. Floyd, Kristin Rose, Pietro De Camilli, Generation of high curvature membranes mediated by direct endophilin bilayer interactions, J. Cell Biol. 155 (2) (2001) 193–200.
- [14] Martina Pannuzzo, Antonio Raudino, Danilo Milardi, Carmelo La Rosa, Mikko Karttunen, α-helical structures drive early stages of self-assembly of amyloidogenic amyloid polypeptide aggregate formation in membranes, Sci. Rep. 3 (2013).
- [15] E. Evans, W. Rawicz, Entropy-driven tension and bending elasticity in condensed-fluid membranes, Phys. Rev. Lett. 64 (17) (1990) 2094.
- [16] Wolfgang Helfrich, Elastic properties of lipid bilayers: theory and possible experiments, Zeitschrift FÜR Naturforschung C 28 (11–12) (1973) 693–703.
- [17] John D. Weeks, Structure and thermodynamics of the liquid-vapor interface, J. Chem. Phys. 67 (7) (1977) 3106–3121.
- [18] W. Helfrich, Out-of-plane fluctuations of lipid bilayers, Zeitschrift Für Naturforschung C 30 (11–12) (1975) 841–842.
- [19] David Boal, David H. Boal, Mechanics of the Cell, Cambridge University Press, 2012
- [20] Scott T. Milner, S.A. Safran, Dynamical fluctuations of droplet microemulsions and vesicles, Phys. Rev. A 36 (9) (1987) 4371.
- [21] Erik Lindahl, Olle Edholm, Mesoscopic undulations and thickness fluctuations in lipid bilayers from molecular dynamics simulations, Biophys. J. 79 (1) (2000) 426–433.
- [22] Himani Agrawal, Liping Liu, Pradeep Sharma, Revisiting the curvature-mediated interactions between proteins in biological membranes, Soft Matter 12 (43) (2016) 8907–8918.
- [23] Osman Kahraman, Peter D. Koch, William S. Klug, Christoph A. Haselwandter, Architecture and function of mechanosensitive membrane protein lattices, Sci. Rep. 6 (2016).
- [24] Xiaojun Liang, Prashant K. Purohit, A fluctuating elastic plate and a cell model for lipid membranes, J. Mech. Phys. Solids 90 (2016) 29–44.
- [25] Xiaojun Liang, Prashant K. Purohit, A fluctuating elastic plate model applied to graphene, J. Appl. Mech. 83 (8) (2016) 081008.
- [26] G. Gompper, D.M. Kroll, Random surface discretizations and the renormalization of the bending rigidity, J. Physique I 6 (10) (1996) 1305–1320.
- [27] F. Fraternali, Gianluca Marcelli, A multiscale approach to the elastic moduli of biomembrane networks, Biomech. Model. Mechanobiol. 11 (7) (2012) 1097– 1108
- [28] Yongli Zhang, Donald M. Crothers, Statistical mechanics of sequence-dependent circular dna and its application for dna cyclization, Biophys. J. 84 (1) (2003) 136–153.
- [29] Tianxiang Su, Prashant K. Purohit, Thermomechanics of a heterogeneous fluctuating chain, J. Mech. Phys. Solids 58 (2) (2010) 164–186.
- [30] Tianxiang Su, Prashant K. Purohit, Fluctuating elastic filaments under distributed loads, Mol. Cell. Biomech. 8 (2011) 215.
- [31] Tianxiang Su, Prashant K. Purohit, Semiflexible filament networks viewed as fluctuating beam-frames, Soft Matter 8 (17) (2012) 4664–4674.
- [32] O. Kahraman, P.D. Koch, W.S. Klug, C.A. Haselwandter, Architecture and function of membrane protein lattices, Sci. Rep. 6 (2015) 19214.
- [33] Klaus-Jürgen Bathe, Finite Element Procedures, Klaus-Jurgen Bathe, 2006.
- [34] Live Rekvig, Bjørn Hafskjold, Berend Smit, Simulating the effect of surfactant structure on bending moduli of monolayers, J. chem. phys. 120 (10) (2004) 4897–4905.